Quantitative Scanning Tunneling Microscopy at Atomic Resolution: Influence of Forces and Tip Configuration

A. R. H. Clarke,[1] J. B. Pethica,[1] J. A. Nieminen,[1,*] F. Besenbacher,[2] E. Lægsgaard,[2] and I. Stensgaard[2]
[1]*Department of Materials, University of Oxford, Parks Road, Oxford, OX1 3PH, United Kingdom*
[2]*Center for Atomic-scale Materials Physics and Institute of Physics and Astronomy, University of Aarhus, DK-8000, Aarhus, Denmark*
(Received 24 July 1995)

Atom resolved scanning tunneling microscopy images are known to depend on the nature of the tip and its interaction with the surface. We present a new method for determining barrier height and tip-surface interactions. For Cu(100) images, two distinct tip types are seen. At larger tunnel currents there is evidence for forces acting between tip and surface. We show that a molecular dynamics simulation of tip and surface is able to quantitatively explain the results, and gives a good estimate of both absolute tip-surface separation and the site dependent forces on individual atoms.

PACS numbers: 61.16.Ch, 73.40.Gk, 73.40.Jn

The remarkable capabilities of scanning tunneling microscopy (STM) and related techniques to image and manipulate atoms are well known [1,2]. The understanding of individual experiments is, however, surprisingly undeveloped. The model of Tersoff and Hamann [3] gives a general picture of STM operation based on topography and local densities of states at the surface. More complex calculations [4] give some insight into the position of adsorbates and possible tip structures. Quantitative modeling of specific images, however, relies on parameters which are not easily determined in experiment. For example, the tip radius and its actual separation from the surface are not directly known. The chemical nature of the tip significantly affects images [5,6], and may even reverse the contrast, yet it is in practice unidentified. Furthermore, forces between tip and surface can play a significant role in STM imaging [7,8] as well as in their more obvious role in atomic-force microscopy (AFM) and in deliberate movement of atoms [9,10]. For quantitative understanding of STM and its applications there is thus considerable interest in experiments which cast light on these phenomena.

An important parameter in STM imaging is the tunnel barrier, or the decay length, κ, normal to the surface. This is experimentally accessible from the variation of tunnel current with tip-surface separation. In practice, accurate measurement of the barrier, particularly at specific atom sites, is quite difficult. Measurements which avoid the displacement compensating effects of the STM feedback loop work either at relatively low speeds, where drift can be a problem, or at high modulation rates, where calibration of the actual piezo displacement can be difficult. In this paper we demonstrate a method which minimizes calibration uncertainties, and uses the imaging mode, for which the STM is by design most accurately calibrated. We measure the variation of image corrugation height with tip-surface separation. Our results provide evidence for two distinct types of tip behavior, likely related to composition. A decrease in corrugation height is observed at higher tunnel currents. We show this can be quantitatively modeled by tip-surface interaction forces, and allows an estimate of true tip-surface separation.

The peak-to-trough height Δ of STM image corrugations at larger tip-surface separations s is given [3] by the expression

$$\Delta \propto \exp(-\beta s)\,, \tag{1}$$

where $\beta = 2(\kappa^2 + 0.25G^2)^{1/2} - 2\kappa$, with $\kappa = (2m_e\Phi)^{1/2}/\hbar$, where Φ is the mean tunnel barrier height, and $G = 2\pi/a$ is the surface reciprocal lattice vector along the direction of interest. Now the variation of tunnel gap conductance σ with separation is dominated by κ [11], and is given by

$$\sigma \propto \exp(-2\kappa s)\,. \tag{2}$$

If the prefactors in Eqs. (1) and (2) are treated as constants, it is easy to show that the corrugation deduced barrier height is given by

$$\Phi_{M,\text{corrugation}} = \frac{\hbar^2 G^2}{8 m_e X}\,, \tag{3}$$

where

$$X = \left(\frac{\partial \ln(\Delta)}{\partial \ln(\sigma)}\right)\left[\frac{\partial \ln(\Delta)}{\partial \ln(\sigma)} + 2\right].$$

Thus the slope in a plot of $\ln(\Delta)$ vs $\ln(\sigma)$ gives a direct measure of Φ. A full analysis allowing for the prefactors in (1) and (2) makes the expression more complex but does not significantly affect the quantitative conclusions. Note that by choosing different surface G vectors, independent measurements of Φ are possible from the same set of images, and by comparing different G directions, insight is gained into the symmetry of tip geometry.

The experiments were performed using a UHV compatible fast scanning STM which has been described elsewhere

 0031-9007/96/76(8)/1276(4)$06.00

[12]. All the STM images were recorded using the constant current mode of operation. The tip was a tungsten single crystal oriented along [100]. Despite exhibiting smaller corrugations, a metal surface was chosen for this study in preference to a semiconductor. The high density of states and its relatively weak variation with voltage minimize the effects of electronic structure on variations in corrugations in the image. Interpretation and modeling is thus more straightforward for metals. A Cu(100) crystal was prepared using sputtering cycles with neon ion bombardment (3 kV, 5 μA) followed by annealing the crystal to 530 °C. Imaging conditions were in the ranges $I = 1-20$ nA and $V = \pm 3-20$ mV. Allowance was made for the 120 kΩ input resistance of the tunnel current amplifier [13]. A typical STM image is shown in Fig. 1.

A key ingredient is that the tip must not change while a set of images is obtained. That the tip remains the same is, however, easily checked in our method by returning to the current used in the first image and ensuring both corrugation height and image features remain the same. Data sets are accepted only where this lack of tip change within the set was carefully confirmed. An interesting general observation is that the corrugation heights were repeatable and reliable within a given data set, but the actual corrugation heights between different data sets varied considerably. For example, typical experimental values for corrugations measured along $\langle 0\bar{1}1\rangle$ were in the range 0.05–0.2 Å. This variability due to differing tips between data sets does not invalidate our analysis, because only the relative variation of the corrugation heights within a single data set is important. A histogram of corrugation heights across different data sets showed two peaks. This suggests that in our experiments there are two generally stable types of tips.

Eighteen data sets, taken over a period of several weeks, were analyzed in detail. Within each data set, the voltage was fixed and the current varied. The individual data points had small standard deviations ($<10\%$ of their measured mean value). Figure 2 shows the results from two sets for corrugations measured along $\langle 0\bar{1}1\rangle$. First there is a linear region at lower values of tunnel current. This can be used to deduce the barrier height in the tunnel gap from the model described above. There is also a "roll-off" region at high tunnel conductance (i.e., at smaller tip-sample separations), typically characterized by a tunnel gap resistance of 0.5–3 MΩ, where the corrugation height does not increase so much with current, and eventually falls with increasing current. This is a clear departure from the Tersoff and Hamman model and a signature of tip-surface interaction. Doyen *et al.* [14] have observed a similar corrugation roll-off in experiments on the clean Au(110) missing row structure. By drawing a best fit line through the linear regime of the data sets in Fig. 2 and substituting the gradient in Eq. (3), the value of the apparent barrier height is found to be 2.05 ± 0.1 eV in the case of the upper data set and 1.9 ± 0.2 eV for the lower set. These values are typical of the data as a whole, which exhibited a range between 1.6 and 2.6 eV with a preponderance of values around 2 eV. The barriers are thus comparable with those obtained by other methods where the STM is giving atomic resolution [15].

The first implication of these results is that we have two types of tips capable of taking high resolution images. McIntyre *et al.* [16] have noted that the corrugation measured for the sulfur $(\sqrt{3} \times \sqrt{3})R30°$ overlayer on Pt(111) dramatically increases upon indenting the tip into the surface and (probably) transferring a sulfur atom onto

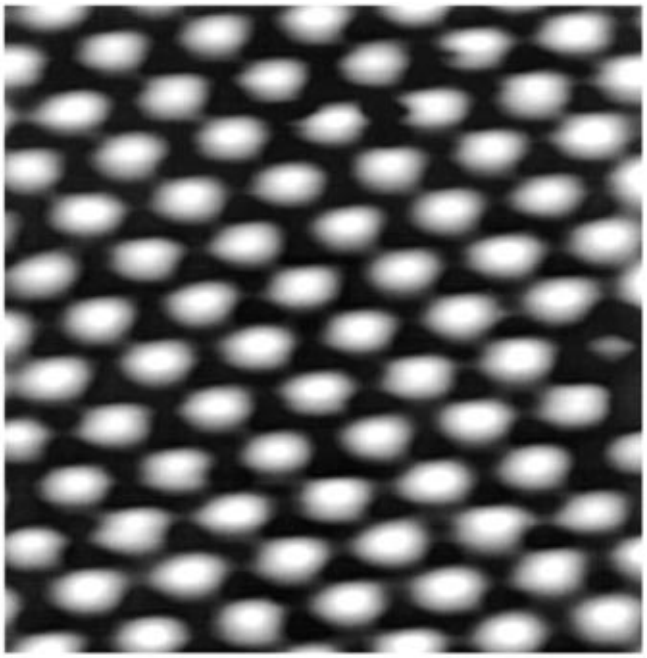

FIG. 1. A 23 Å $\times$ 23 Å image of Cu(100) taken at 12.5 nA and 28 mV. The defect shows the tip is sharp.

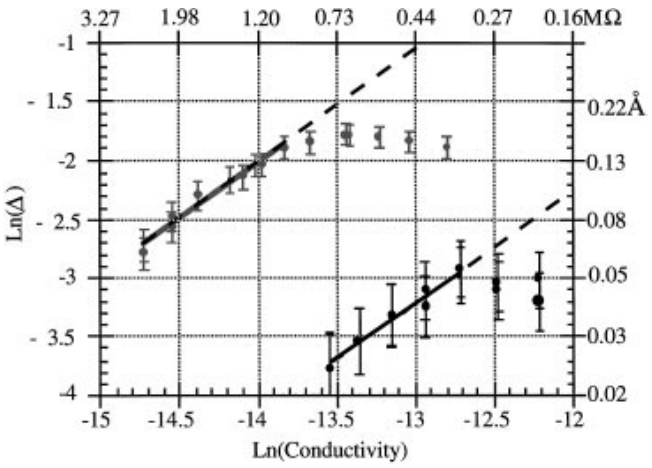

FIG. 2. $\ln(\Delta)$ vs $\ln(s)$ plots illustrating the two general types of tips obtained in this work. Tunnel voltage: 3 mV for upper and 4 mV for lower plot.

the tip apex. Our higher corrugation data might thus be associated with a nonmetal atom adsorbed at the tip apex, while the lower corrugation height data might be due to a metallic atom adsorbed at the tip. Ruan *et al.* [6] have also shown that by varying the chemical species between a metallic and a nonmetallic atom at the apex the image contrast is strongly affected. Surprisingly, however, there was no obvious correlation between the variation of barrier between different data sets and the variation of corrugation heights. If there is a different chemical species at the tip for the two broadly different groups as suggested above, then it does not obviously affect the tunnel barrier. We conclude therefore that difference of tip geometry (that is, of effective tip radius) rather than chemical composition is more likely to be the cause of the two groups of corrugation height.

From the roll-off region of the data in Fig. 2 at higher tunnel currents, it is clear that additional interactions have a role to play in the formation of STM images. The key to understanding their effect is that when forces start to act the relative movement of the tip apex and surface atoms is no longer the same as that of more distant parts of tip and sample where the displacements are experimentally measured [7]. Ciraci, Baratoff, and Batra [17] showed how forces can give rise to reduced image corrugation. To evaluate these concepts in a modeling experiment we have made a molecular dynamics calculation of the relative displacements for a Cu tip and surface. Full details of the method are given elsewhere [18]. In this simulation there are 676 atoms in the tip and 768 in the surface. The surface normal is (100) and the tip has the same alignment. Sutton-Chen potentials [19] are used for the interatomic forces. Figure 3 shows the actual displacement of the tip apex atom above the plane of the surface topmost atoms versus relative displacement of points far from the tunnel zone. Curves are shown for two lateral positions of the apex atom, one over the fourfold hollow site, the other "on top" of a surface atom.

At large separations, the forces are small, so the two displacements are virtually the same, as expected. At smaller separations, the far field displacement becomes less than the actual tip atom motion, since the tip atom is attracted towards the surface. The measured image corrugation will therefore fall below the true corrugation motion of the tip atom, which is the roll-off that we observe in the experiments. The falloff in corrugation may be calculated from the molecular dynamics (MD) data. A given tip atom corrugation in the $\langle 010 \rangle$ direction, for example, is converted to measured corrugation by finding the far field displacement for the hollow site at corrugation minima (closest approach to surface), and for the on-top site at maxima. See the graphical construction in Fig. 3. Similarly, the bridge site and on-top site results are used for the $\langle 0\bar{1}1 \rangle$ direction data.

To make the comparison with experiment, it is necessary to relate current changes to displacements. *Changes* in displacements are easily calculated from Eq. (2) using the experimental value of the barrier height. Thus the true (tip atom) corrugations are obtained from the straight line section of Fig. 2 and its extrapolation to smaller separations. However, use of Eq. (2) to determine *absolute* separation is far too dubious a procedure. Even if the tip geometry and composition were known, the calculation of actual tunnel currents is problematic. Therefore we reverse the argument—absolute separation is set by a simple shift of the separation to give a best fit between the MD prediction of roll-off and experiment. In other words, we determine the absolute separation of the tip and the surface atom avoiding use of the absolute value of the tunnel current. Note this does not mean there is any arbitrariness in the separation axis scale. The agreement of model and experiment is seen to be good (Fig. 4) and gives a remarkably sensitive determination of separation which avoids the serious uncertainties involved in making full physical tip contact (crash) to determine zero of separation.

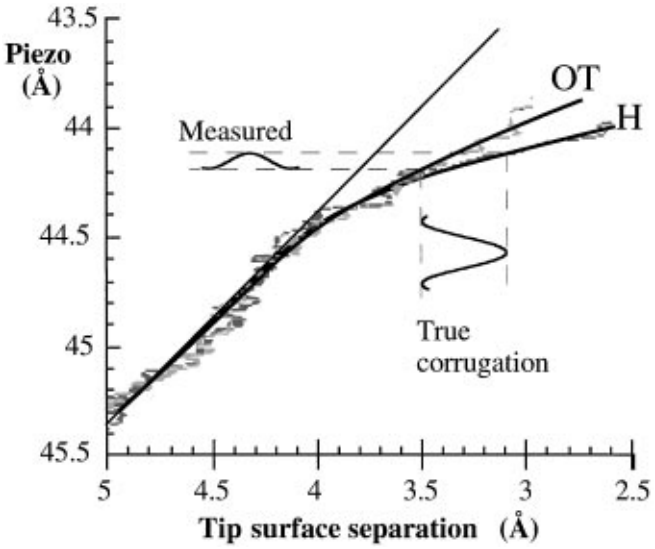

FIG. 3. Molecular dynamics calculation of displacement of tip atom above surface atom plane relative to that of points farther away from tip. OT is tip above a surface atom (on top) and H is above a fourfold hollow in the Cu(100) surface. Bridge sites show an intermediate behavior.

The calculations show that the force between the tip and the sample is around 1 nN at a separation of 3.5 Å, in good agreement with the measurements of Dürig, Zuger, and Pohl [20]. It varies by roughly 6% between hollow and on-top sites. Also at this separation the measurable stiffness varies by roughly 1 N/m between the sites, which suggests that atomic resolution AFM based on compliance measurement is possible. However, the absolute separations are very small, and rather close to instability. Use in the simulation of different chemical species at the tip apex will give other force constants, and may provide a means of characterizing the bond and surface interaction; the technique presented here is in a

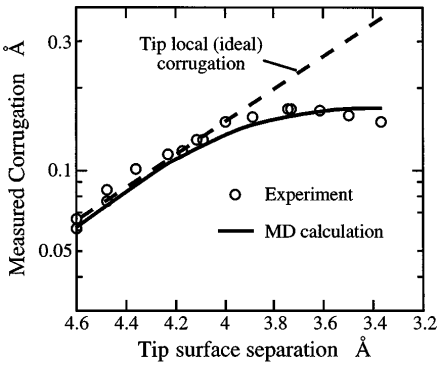

FIG. 4. Comparison of experiment roll-off in corrugation (top data of Fig. 2) with that deduced from the molecular dynamics calculations.

sense a combination of STM and AFM. Although our results imply that atomistic calculations may be necessary for each material species studied, they also offer an explanation for the wide quantitative variety of STM images observed in practice.

We have, of course, ignored the possibility of significant change in density of states (DOS) near to the Fermi level, as the tip and surface start to interact. Doyen *et al.* [14] suggested this was the cause of the roll-off in corrugations they observed. However, we note that the force mechanism we propose acts at almost 1 Å greater separation than the DOS changes found by Doyen *et al.*, and so should be a dominant effect. It is also a universal mechanism which occurs for all tip species. Furthermore, the required substantial changes in DOS due to the proximity of the tip might not easily occur for many metal crystal faces.

In summary, we have shown that a straightforward measurement of corrugation height variation with tunnel current can give significant insight into imaging mechanisms. For our experiments on Cu(100) we observe two types of tip, most likely due to different tip atom geometric arrangement. We also show that image corrugations fall off at small tunnel resistances, and that this may be quantitatively explained by forces acting between tip and surface. In particular, we can estimate true tip-surface separation, and the force variation between sites. The new measurement technique provides a method of assessing forces before they induce actual motion of atoms at surfaces, and could therefore provide insight into the critical early stages of atomic manipulation.

A. R. H. C. thanks EPSRC (UK) for financial support. This work was supported by the Danish National Research Foundation via the Center for Atomic-scale Materials Physics. Discussions with Dr. A. P. Sutton are gratefully acknowledged.

*Permanent address: Department of Physics, Tampere University of Technology, P.O. Box 692, SF-33101, Tampere, Finland.

[1] R. J. Behm, in *Scanning Tunnelling Microscopy and Related Methods*, edited by R. J. Behm, N. Garcia, and H. Rohrer (Kluwer Academic Publishers, Dordrecht, 1990), pp. 173–209.
[2] J. A. Stroscio and D. M. Eigler, Science **252**, 1319 (1991).
[3] J. Tersoff and D. R. Hamann, Phys. Rev. Lett. **50**, 1998 (1983).
[4] P. Sautet *et al.*, Surf. Sci. **315**, 127 (1994).
[5] M. Schmidt, H. Stadler, and P. Varga, Phys. Rev. Lett. **70**, 1441 (1993).
[6] L. Ruan, F. Besenbacher, I. Stensgaard, and E. Lægsgaard, Phys. Rev. Lett. **70**, 4079 (1993).
[7] J. H. Coombs and J. B. Pethica, IBM J. Res. Dev. **30**, 455 (1986); J. B. Pethica, Phys. Rev. Lett. **57**, 3235 (1986).
[8] J. Winterlin *et al.*, Phys. Rev. Lett. **62**, 59 (1989).
[9] D. M. Eigler and E. K. Schweitzer, Nature (London) **344**, 524 (1990).
[10] G. Binnig, C. F. Quate, and Ch. Gerber, Phys. Rev. Lett. **56**, 930 (1986).
[11] C. J. Chen, *Introduction to Scanning Tunnelling Microscopy* (Oxford University Press, New York, 1993).
[12] L. Eirdal *et al.*, Surf. Sci. **312**, 39 (1994).
[13] L. Olesen *et al.*, Phys. Rev. Lett. **72**, 2251 (1994).
[14] G. Doyen *et al.*, Phys. Rev. B **48**, 1738 (1993).
[15] R. Schuster *et al.*, Ultramicroscopy **42–44**, 533 (1992); J. Knall, J. H. Wilson, and J. B. Pethica, Institute of Physics Conf. Ser., London **134**, 597 (1993).
[16] B. J. McIntyre *et al.*, J. Vac. Sci. Technol. B **12**, 1751 (1994).
[17] S. Ciraci, A. Baratoff, and I. P. Batra, Phys. Rev. B **42**, 7618 (1990).
[18] A. P. Sutton, J. B. Pethica, H. Rafii-Tabar, and J. A. Nieminen, in *Electron Theory in Alloy Design*, edited by D. G. Pettifor and A. H. Cottrell (The Institute of Materials, London, 1992), pp. 191–223.
[19] A. P. Sutton and J. Chen, Philos. Mag. Lett. **61**, 13 (1990).
[20] U. Dürig, O. Züger, and D. W. Pohl, J. Microsc. **152**, 259 (1988).